

# Quantitative assessment of right ventricular function and pulmonary regurgitation in surgically repaired tetralogy of Fallot using 256-slice CT: comparison with 3-Tesla MRI

Yuzo Yamasaki · Michinobu Nagao · Kenichiro Yamamura · Masato Yonezawa · Yoshio Matsuo · Satoshi Kawanami · Takeshi Kamitani · Ko Higuchi · Ichiro Sakamoto · Yuichi Shiokawa · Hidetake Yabuuchi · Hiroshi Honda

Received: 2 February 2014 / Revised: 24 June 2014 / Accepted: 11 July 2014 / Published online: 12 August 2014  
© European Society of Radiology 2014

## Abstract

**Objectives** To compare 256-slice cardiac computed tomography (CCT) with cardiac magnetic resonance (CMR) imaging to assess right ventricular (RV) function and pulmonary regurgitant fraction (PRF) in patients with repaired tetralogy of Fallot (TOF).

**Methods** Thirty-three consecutive patients with repaired TOF underwent retrospective ECG-gated CCT and 3-Tesla CMR. RV and left ventricular (LV) end-diastolic volume (EDV), end-systolic volume (ESV), stroke volume (SV) and ejection fraction (EF) were measured using CCT and CMR. PRF-CCT (%) was defined as  $(RVS\!V - LV\!S\!V) / RVS\!V$ . PRF-CMR (%) was measured by the phase-contrast method. Repeated measurements were performed to determine intra- and interobserver variability.

Y. Yamasaki · M. Yonezawa · Y. Matsuo · T. Kamitani · K. Higuchi · H. Honda  
Department of Clinical Radiology, Graduate School of Medical Sciences, Kyushu University, 3-1-1 Maidashi, Higashi-ku, Fukuoka 812-8582, Japan

M. Nagao (✉) · S. Kawanami  
Department of Molecular Imaging & Diagnosis, Graduate School of Medical Sciences, Kyushu University, 3-1-1 Maidashi, Higashi-ku, Fukuoka 812-8582, Japan  
e-mail: minagao@radiol.med.kyushu-u.ac.jp

K. Yamamura  
Department of Pediatrics, Graduate School of Medical Sciences, Kyushu University, 3-1-1 Maidashi, Higashi-ku, Fukuoka 812-8582, Japan

I. Sakamoto  
Department of Cardiovascular Medicine, Graduate School of Medical Sciences, Kyushu University, 3-1-1 Maidashi, Higashi-ku, Fukuoka 812-8582, Japan

Y. Shiokawa  
Department of Cardiovascular Surgery, Graduate School of Medical Sciences, Kyushu University, 3-1-1 Maidashi, Higashi-ku, Fukuoka 812-8582, Japan

H. Yabuuchi  
Department of Health Sciences, Graduate School of Medical Sciences, Kyushu University, 3-1-1 Maidashi, Higashi-ku, Fukuoka 812-8582, Japan

**Results** CCT measurements, including PRF, correlated highly with the CMR reference ( $r=0.71-0.96$ ). CCT overestimated RVEDV (mean difference,  $17.1 \pm 2.9$  ml), RVESV ( $12.9 \pm 2.1$  ml) and RVS $V$  ( $4.2 \pm 2.0$  ml), and underestimated RVEF ( $-2.6 \pm 1.0$  %) and PRF ( $-9.1 \pm 2.0$  %) compared with CMR. The limits of agreement between CCT and CMR were in a good range for all measurements. The variability in CCT measurements was lower than those in CMR. The estimated effective radiation dose was  $7.6 \pm 2.6$  mSv.

**Conclusions** 256-slice CCT can assess RV function and PRF with relatively low dose radiation exposure in patients with repaired TOF, but overestimates RV volume and underestimates PRF.

## Key points

- 256-slice CT assessment of RV function is highly reproducible in repaired TOF.
- Pulmonary regurgitation can be evaluated by biventricular systolic volume difference.
- CT overestimates RV volume and underestimates pulmonary regurgitation, compared with MRI.

**Keywords** Tetralogy of Fallot · Right ventricular function · Pulmonary regurgitation · Multislice computed tomography · Magnetic resonance imaging

## Abbreviations

CCT	Cardiac computed tomography
CMR	Cardiac magnetic resonance
CHD	Congenital heart disease
ECG	Electrocardiogram
EDV	End-diastolic volume
EF	Ejection fraction
ESV	End-systolic volume
HU	Hounsfield units
LV	Left ventricle/ventricular
PR/PRF	Pulmonary regurgitation/pulmonary regurgitant fraction
ROI	Region of interest
RV	Right ventricle/ventricular
SV	Stroke volume
TOF	Tetralogy of Fallot

## Introduction

In patients with surgically repaired tetralogy of Fallot (TOF), residual pulmonary regurgitation (PR) is an important determinant of outcome, as it may contribute to right ventricular (RV) enlargement and dysfunction. Furthermore, these changes may result in exercise intolerance, a propensity for arrhythmias and an increased risk of sudden cardiac death. Previous studies reported that RV volume or ejection fraction can be used as an index of RV dysfunction, and that severe PR was the most common indication for reoperation in patients with repaired TOF [1–4].

Cardiac magnetic resonance (CMR) is the current reference standard to evaluate RV performance and PR, owing to its ability to quantify ventricular volumes and pulmonary arterial flow [5–8]. CMR is non-invasive and does not expose the patient to ionizing radiation. Nevertheless, CMR is contraindicated in patients with an implanted pacemaker/defibrillator, patients with claustrophobia or any clinical condition that prohibits a long CMR examination. Therefore, echocardiography and cardiac computed tomography (CCT) are used in these patients [9]. However, echocardiographic assessment of RV function is also limited because of complex RV geometry [5]. Furthermore, Doppler echocardiographic assessment of PR is dependent on the observer's experience, and is limited by post-operative structural changes. CCT has recently undergone major technological developments that currently allow quantification of cardiac function with low dose radiation exposure. The unprecedented quality of CCT images, which offer superb endocardial definition optimal for boundary detection, suggests that this modality could potentially constitute a more reproducible reference technique. Moreover, the incremental value of concomitant assessment of cardiac function in

addition to coronary artery morphology by CCT has been recognized [10].

A previous study demonstrated good correlations between CCT and CMR measurements of right ventricular functional parameters in patients with ischemic cardiomyopathy [11, 12]. However, in patients with repaired TOF, the accuracy and reproducibility of assessing RV function with CCT have not been examined. Furthermore, the accurate assessment of PR is important in managing patients with repaired TOF, but CCT cannot directly evaluate PRF. In the present study, we attempted to quantify PR using biventricular stroke volume data obtained from CCT. Thus, the purpose of this study was to investigate the accuracy and reproducibility of RV function and PR measurements with 256-slice CCT in patients with repaired TOF using CMR measurements as the reference standard.

## Materials and methods

### Study population

Between June 2010 and November 2013, we prospectively enrolled 33 consecutive patients with surgically repaired TOF. All patients underwent both CCT and CMR for the assessment of cardiac function within 1 week at our hospital. CCT and CMR were performed on the same day in 21 patients and within 1 week in 12 patients. Patients' characteristics are shown in Table 1. General exclusion criteria for contrast CT studies were renal insufficiency, severe arrhythmia (e.g. atrial fibrillation), pregnancy and history of contrast media reaction. Exclusion criteria for CMR were an implanted cardiac pacemaker or defibrillator or other MR-unsafe ferromagnetic objects and claustrophobia. The study was approved by our institutional review board and written informed consent was obtained from each patient prior to imaging.

**Table 1** Patient characteristics

Characteristics	Value
Total	33
Age	28.9±13.1
Male/female	19/14
BSA (m <sup>2</sup> )	1.5±0.3
Age of corrective surgery	5.7±6.8
NYHA functional classification I/II/III/IV	25/8/0/0
BNP	56.1±42.7

Data are presented as mean±standard deviation or number of patients  
*BSA* body surface area, *NYHA* New York Heart Association, *BNP* brain natriuretic peptide

## 256-slice CCT

All CCT examinations were performed using a 256-MSCT system (Brilliance iCT; Philips Healthcare, Cleveland, OH, USA). All patients underwent retrospective electrocardiogram (ECG)-gated helical examinations with ECG tube current modulation. The detector collimation was  $2 \times 128 \times 0.625$  mm with a dynamic z-focal spot, resulting in a sample collimation of 256 simultaneous slices of 0.625 mm thickness. The tube voltage was 80 or 100 kV. To improve image quality, reduced-dose scan series were reconstructed using an iterative reconstructive technique (iDose4, Philips Healthcare, Cleveland, OH, USA). Images were reconstructed with an individually adapted field of view encompassing the heart in a matrix of  $512 \times 512$  pixels, the cardiac standard convolution kernel and a section thickness of 2 mm with an increment of 1 mm. No additional beta-blocker or nitroglycerin was administered to avoid influencing cardiac function. For all patients, an iodinated contrast agent (Iopamidol, 370 mg I/ml; Bayer Healthcare, Osaka, Japan) was administered at a volume based on the patient's weight. The contrast agent was injected over 13 s and was followed by the injection of contrast agent diluted 1:1 with saline for 10 s as a chaser. The contrast agent and chaser were injected at a rate of 0.7 ml/kg/s into the antecubital vein via a 20-gauge catheter using a dual-head injector. Automatic bolus tracking was performed with the region of interest (ROI) placed in the aortic root. All CCT scans were initiated 5 s after the mean ROI contrast reached a predetermined threshold of 200 Hounsfield units (HU) at a tube voltage of 100 kV or 230 HU at a tube voltage of 80 kV.

## Cardiac MRI

All patients underwent 3-Tesla MR imaging (Achieva 3.0 T Quasar Dual; Philips Healthcare, Best, the Netherlands) equipped with dual-source parallel radiofrequency transmission, 32-element cardiac phased-array coils used for radiofrequency reception and a four-lead vectorcardiogram used for cardiac gating. Cine-balanced turbo field-echo sequences in axial view images and short-axis view images acquired in parallel to the atrioventricular groove from the base to apex were performed with the following imaging parameters: repetition time 2.8 ms, echo time 1.4 ms, flip angle  $45^\circ$ , slice thickness 8 mm, field of view 380 mm, matrix size  $176 \times 193$ , SENSE factor 2, 20 cardiac phases/RR intervals of the ECG. Phase contrast velocity mapping with a flow-sensitive, gradient-echo sequence was performed in the main pulmonary artery to assess the pulmonary regurgitant fraction (PRF) (Fig. 1). Imaging parameters were as follow: repetition time 6.2 ms, echo time 3.9 ms, flip angle  $10^\circ$ , velocity encoded value (VENC) set to 100–250 cm/s, slice thickness 3 mm, field of view  $320 \times 300$ , matrix size  $128 \times 256$ , 30 cardiac phases/RR intervals of the ECG.

## CCT and MRI data analysis

Image reconstruction of CCT was retrospectively gated to the ECG; 10 phases were reconstructed throughout the cardiac cycle, with the RR interval divided into 10 % increments. One experienced radiologist (over 5 years' clinical experience in cardiac radiology) who was blinded to the patient's clinical information evaluated the CCT and CMR data sets and determined RV and LV end-diastolic volume (EDV), end-systolic volume (ESV), stroke volume (SV) and ejection fraction (EF).

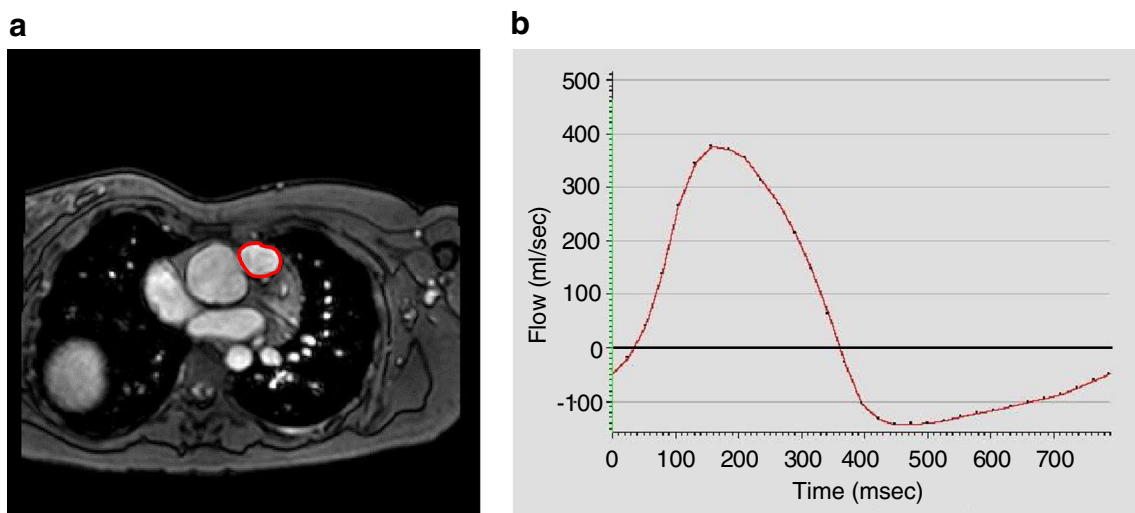


**Fig. 1** **a** Phase-contrast imaging in a patient with repaired TOF and PR. Cine image from a phase-contrast sequence shows the pulmonary artery (rounded red line) in cross section. **b** Graph illustrates flow (ml/s) versus

time (ms) during phase-contrast imaging. PR is the ratio of retrograde flow volume (regurgitation) to antegrade flow volume (ml)

All volumes were indexed to body surface area. End-diastolic and end-systolic phases were identified visually on those images showing the largest and smallest left and right ventricular cavity areas, respectively. Ventricular volumes were measured on CCT based on axial images using a workstation (Extended Brilliance Workspace, Philips Healthcare, Cleveland, OH, USA). CCT images were analysed semi-automatically, followed by manual correction (Fig. 2). CMR images were measured using a workstation (Extended Workspace, Philips Healthcare, Cleveland, OH, USA). CMR images were analysed semi-automatically, followed by manual correction. RV volumes were measured on the basis of axial images (Fig. 3a, b), as previously reported [13]. LV volumes were measured on the basis of short-axis images (Fig. 3c, d). Papillary muscles, moderator bands and trabeculations were assigned to the intracavitary lumen of the ventricles.

PRF-CCT (%) was defined as the difference between RV and LV stroke volume divided by RV stroke volume using CCT volumetric data. When PRF-CCT was a negative value, it was assigned a value of zero. Patients with more than trivial regurgitation of the atrioventricular or aortic valves, or significant residual shunt were excluded from the calculation of pulmonary regurgitant fraction by stroke volume difference.

### Reproducibility

In 15 randomly selected patients, image analysis was repeated at least 1 month later by the same primary reader and by an additional reader (with over 5 years' clinical experience in cardiac radiology) who was blinded to the results of the initial study to determine the reproducibility of measurements for each imaging modality. The reproducibility of the CCT- and CMR-derived measurements was evaluated by calculating the

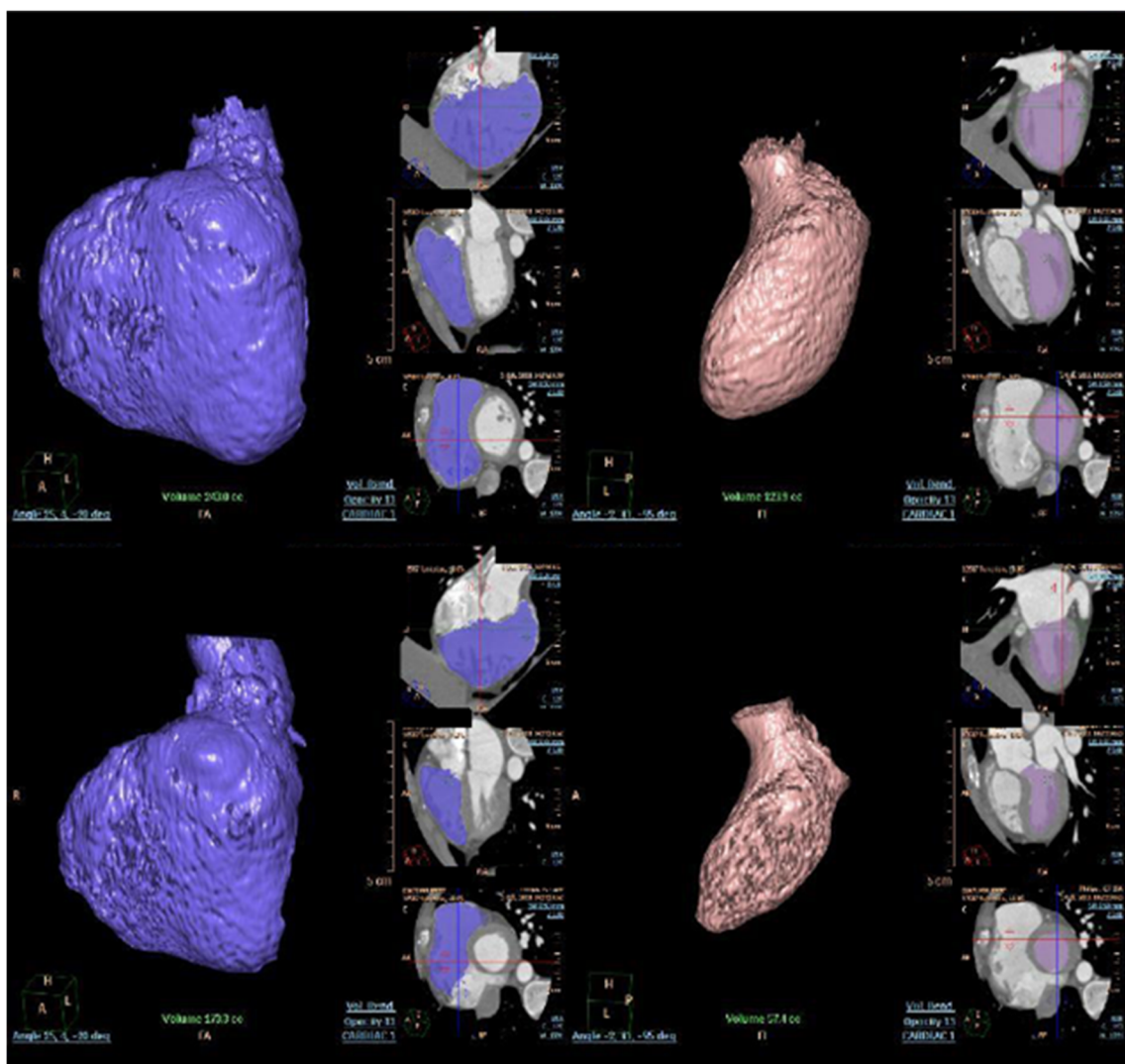
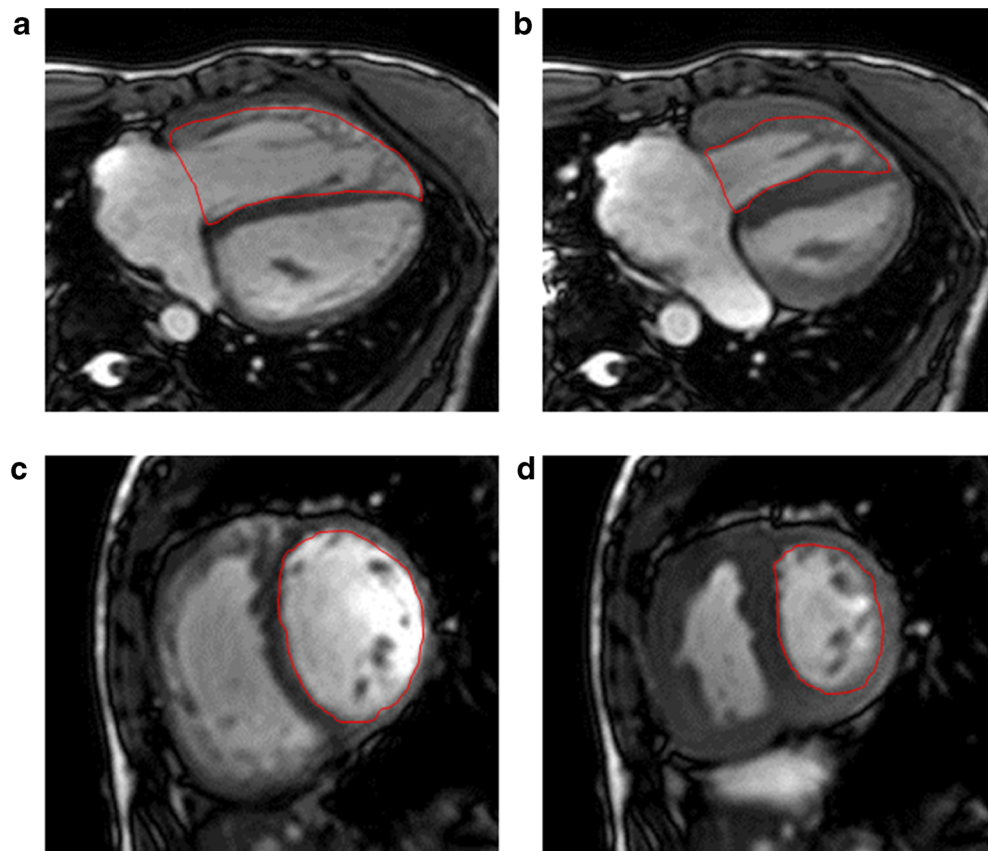


**Fig. 2** Post-processing screen illustrates the single step used to measure RV end-diastolic volume (*upper left*), RV end-systolic volume (*lower left*), LV end-diastolic volume (*upper right*) and LV end-systolic volume (*lower right*) from a CCT data set



**Fig. 3** **a** Cine axial image at the end-diastolic phase to measure RVEDV. **b** Cine axial image at the end-systolic phase to measure RVESV. **c** Cine short-axis image at the end-diastolic phase to measure LVEDV. **d** Cine short-axis image at the end-systolic phase to measure LVESV



inter- and intraobserver variability, defined as the absolute value of the difference between each pair of measurements (by the same observer or different observers) divided by the mean of the measurement pair (expressed as a percentage).

#### Statistical analysis

Data are presented as means±SDs. A paired *t* test was applied to assess the differences between CCT and CMR parameters. The relationship between CCT and CMR was tested by two-variable linear regression analysis, with Pearson's correlation coefficient. Bland–Altman analysis was used to further determine the agreement between CCT and CMR values by calculating the bias (mean difference) and the 95 % limits of agreement ( $\pm 1.96 \times$  SD of the mean difference). All statistical analyses were performed using JMP software (Version 9.0.2), with *p* values less than 0.05 considered statistically significant.

#### Results

During acquisition of CCT data, all patients had regular sinus rhythm, and the mean heart rate was  $70 \pm 11$  beats per minute (bpm) (range, 54–96 bpm). The tube voltage was 80 kV for 14 patients and 100 kV for 19 patients. The estimated effective

radiation dose was  $7.6 \pm 2.6$  mSv (range, 3.7–11.4 mSv). The image noise for LV and RV cavities, determined as the SD of the attenuation value in a single round ROI, was  $27.7 \pm 9.3$  HU (range, 11.9–41.3 HU) and  $27.7 \pm 10.2$  HU (range, 11.1–46.7 HU), respectively.

#### Correlations between CCT and CMR measurements

##### *Right ventricular function*

The mean RVEDV, RVESV, RVSV and RVEF measured by CCT and CMR are summarized in Table 2. Mean RVEDV and RVESV measured on CCT were significantly higher compared to CMR (CCT vs. CMR: RVEDV  $164.4 \pm 59.1$  vs.  $147.3 \pm 53.8$  ml, RVESV  $93.0 \pm 39.7$  vs.  $80.0 \pm 37.3$  ml;  $p < 0.001$ ). Mean RVSV derived from CCT images were slightly but nevertheless significantly higher compared to CMR (CCT vs. CMR:  $71.5 \pm 25.0$  vs.  $67.3 \pm 21.9$  ml;  $P < 0.05$ ). Mean RVEF derived from CCT images were slightly but nevertheless significantly lower compared to CMR (CCT vs. CMR:  $44.2 \pm 7.7$  vs.  $46.8 \pm 7.5$  %;  $P < 0.05$ ). The Pearson correlation coefficients between CMR and CCT measurements of RV function were good ( $r = 0.71$ – $0.96$ ) (Table 2, Fig. 4). The limits of agreement between CCT and CMR were in a good range for all measurements (Fig. 5).

**Table 2** Cardiac function by CCT compared to CMR ( $n=33$ )

	CCT	CMR	Paired <i>t</i> test ( <i>p</i> )	Pearson's coefficient ( <i>r</i> )
RVEDV (ml/m <sup>2</sup> )	164.4±59.1	147.3±53.8	<0.001	0.96*
RVESV (ml/m <sup>2</sup> )	93.0±39.7	80.0±37.3	<0.001	0.95*
RVSV (ml/m <sup>2</sup> )	71.5±25.0	67.3±21.9	0.04	0.90*
RVEF (%)	44.2±7.7	46.8±7.5	0.02	0.71*
LVEDV (ml/m <sup>2</sup> )	97.4±31.9	92.9±30.1	0.02	0.95*
LVESV (ml/m <sup>2</sup> )	45.7±21.3	44.5±18.9	0.40	0.92*
LVSV (ml/m <sup>2</sup> )	51.6±15.5	47.9±14.8	0.01	0.89*
LVEF (%)	53.9±8.7	52.6±6.8	0.23	0.73*

Data are mean±standard deviation;  $n$  = number of patients

CCT cardiac computed tomography, CMR cardiac magnetic resonance, *RV* right ventricle, *LV* left ventricle, *EDV* end-diastolic volume, *ESV* end-systolic volume, *SV* stroke volume, *EF* ejection fraction

\* $p<0.0001$

### Left ventricular function

The mean LVEDV, LVESV, LVSV and LVEF measured by CCT and CMR are summarized in Table 2. Mean LVEDV and LVSV measured on CCT were significantly higher compared to CMR (CCT vs. CMR: LVEDV 97.4±31.9 vs. 92.9±30.1 ml, LVSV 51.6±15.5 vs. 47.9±14.8 ml;  $p<0.05$ ). Mean LVESV and LVEF measured on CCT were slightly higher compared to CMR, as reflected by nonsignificant biases of 1.3 ml and 1.3 %, respectively (CCT vs. CMR: LVESV 45.7±21.3 vs. 44.5±18.9 ml,

LVEF 53.9±8.7 vs. 52.6±6.8 %;  $p>0.05$ ). The Pearson correlation coefficients between CMR and CCT measurements of LV function were good ( $r=0.73$ – $0.95$ ) (Table 2, Fig. 6). The limits of agreement between CCT and CMR were in a good range for all measurements (Fig. 7).

### Pulmonary regurgitation

In three patients, PRF analysis using phase-contrast MRI could not be performed because of susceptibility artefacts from sternal wires or implants. Three patients

**Fig. 4** Scattergram shows the results of linear regression analysis between CCT and CMR measurement of RVEDV (a), RVESV (b), RVSV (c) and RVEF (d) for all patients. The regression equation and Pearson's correlation coefficient are provided for each plot

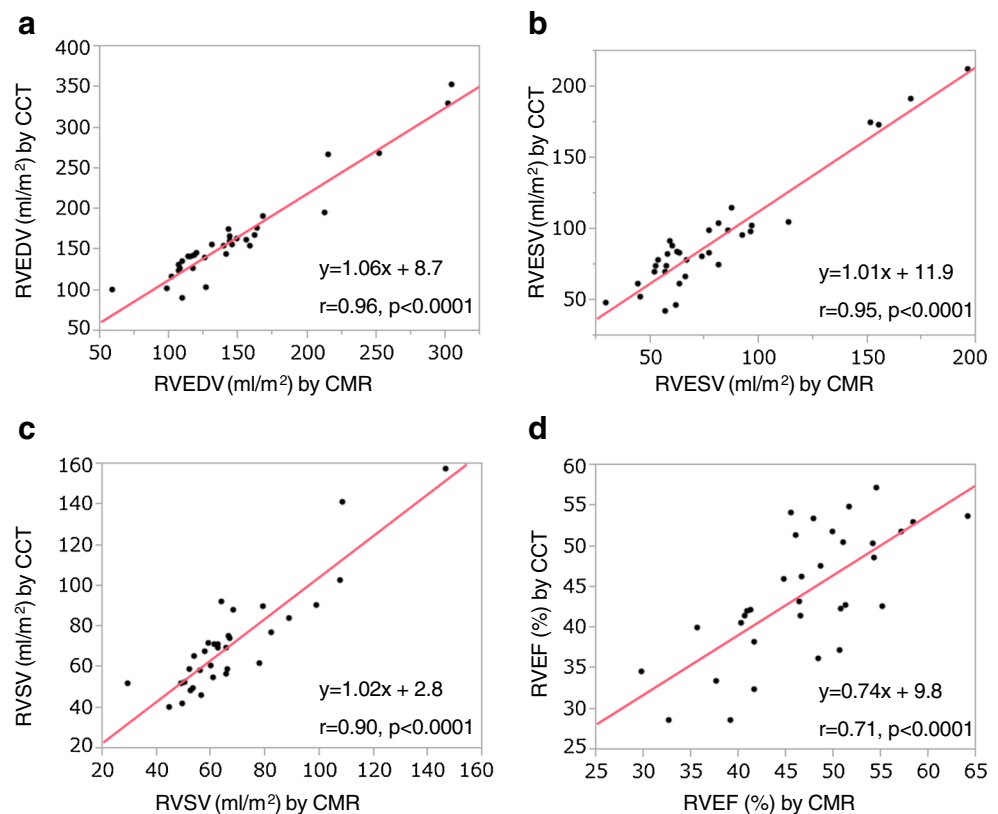
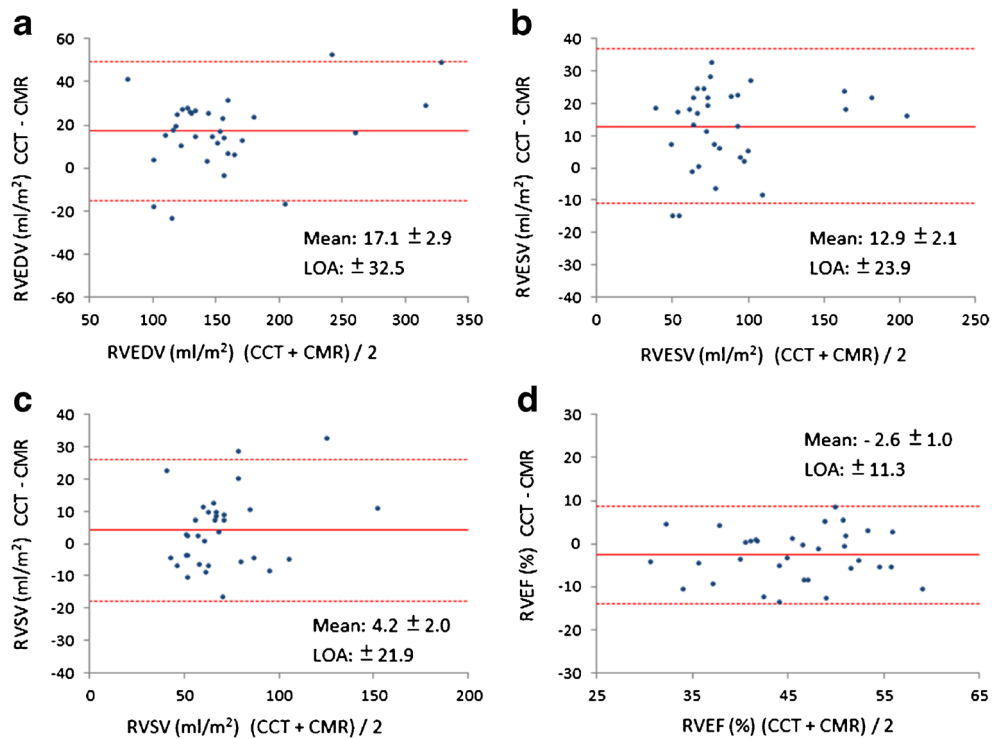


**Fig. 5** Bland–Altman plots show degree of agreement between CCT and CMR of RVEDV (a), RVESV (b), RVSV (c) and RVEF (d) for all patients. The solid line represents mean difference. The broken line represents the 95 % limits of agreement (LOA) ( $\pm 1.96 \times SD$ ). The Bland–Altman analysis show overestimation of RVEDV and RVESV and close agreement of the two methods for RVSV and RVEF



had moderate or severe valvular insufficiency of aortic or mitral valve, one patient had a partial anomalous pulmonary venous return and one patient had large major aortopulmonary collateral arteries. A total of eight

patients were excluded from the pulmonary regurgitation analysis.

The PRF values measured by both MRI and CT in 25 patients are shown in Table 3. There was an excellent

**Fig. 6** Scattergram shows results of linear regression analysis between CCT and CMR measurement of LVEDV (a), LVESV (b), LVSV (c) and LVEF (d) for all patients. The regression equation and Pearson’s correlation coefficient are provided for each plot

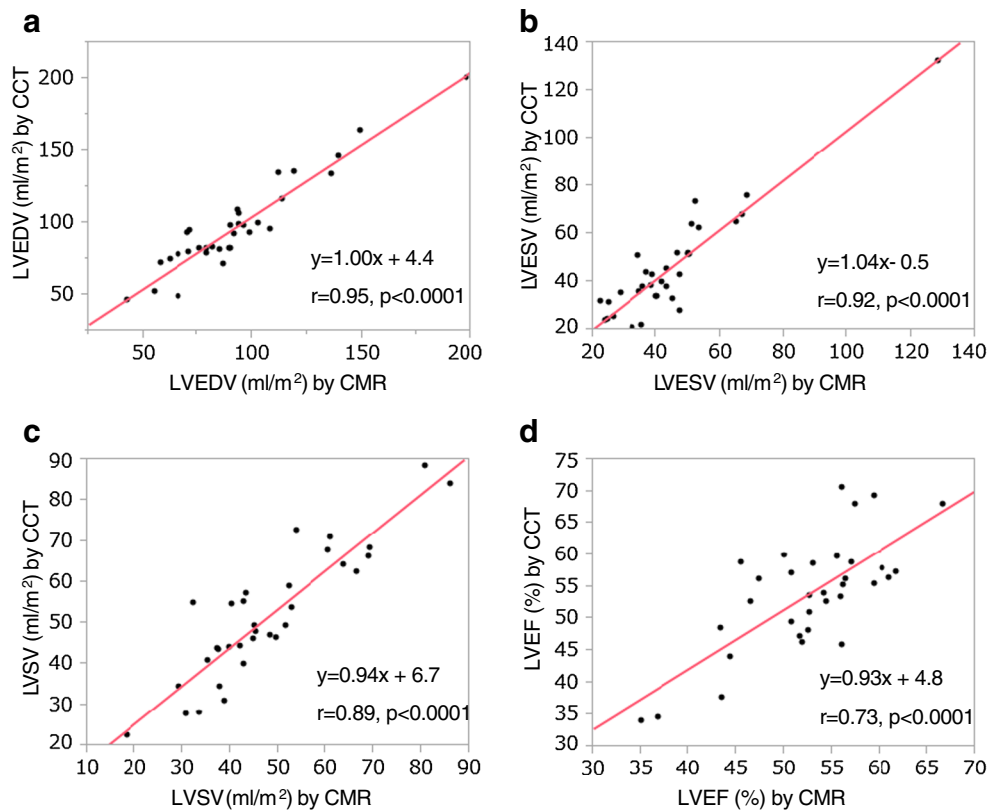
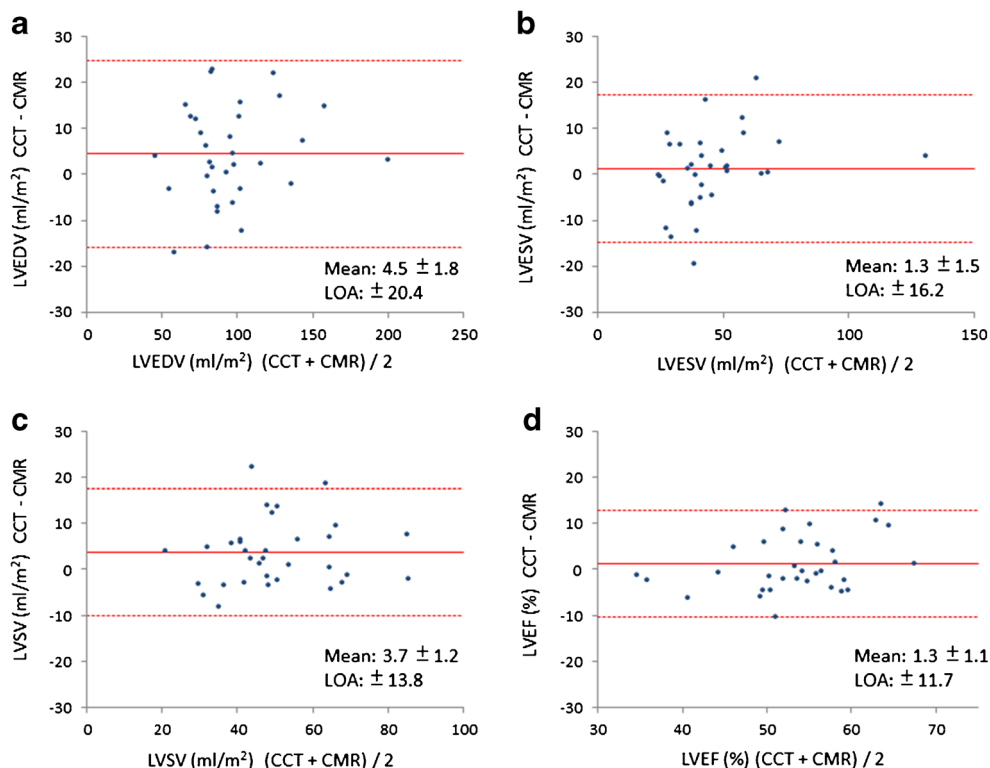


**Fig. 7** Bland–Altman plots show the degree of agreement between CCT and CMR measurement of LVEDV (a), LVESV (b), LVSV (c) and LVEF (d) for all patients. The *solid line* represents mean difference. The *broken line* represents the 95 % limits of agreement (LOA) ( $\pm 1.96 \times \text{SD}$ ). The Bland–Altman analysis shows close agreement with little bias between the two methods for the measurement of LV function



correlation between PRF-CCT and PRF-CMR ( $r=0.90$ ,  $p<0.0001$ ) (Table 3, Fig. 8a). CCT significantly underestimated PRF compared with MRI (mean difference,  $-9.1 \pm 2.0$  %) (Fig. 8b). The limits of agreement ( $\pm 1.96 \times \text{SD}$  of the mean difference) between the two modalities were 9.7 to  $-27.9$  %.

#### Intra- and interobserver variability

Inter- and intraobserver variability data for the cardiac function measurements obtained by CCT and CMR are summarized in Table 4. Both the inter- and intraobserver variability values for the functional parameters were lower with CCT than with CMR.

## Discussion

Advances in medical treatment, cardiac surgery, intensive care and non-invasive diagnosis over the last 50 years have led to

enormous worldwide growth in the number of adults with congenital heart disease (CHD) [14]. The prevalence of CHD in adults and the median age of patients with severe CHD have increased in the general population. In 2000, there were nearly equal numbers of adults and children with severe CHD [15]. Patients with TOF following surgical repair represent a growing population with congenital heart disease, as they now survive into adulthood. Non-invasive modalities to assess cardiac function in these patients will become more important.

Our results confirmed the linear relationship between CCT and CMR, as reflected by the high correlation coefficients obtained for RV and LV functions (Table 2; Figs. 4, 6). CCT measurements were found to be highly reproducible, as reflected by lower inter- and intraobserver variability in all measurements. Meanwhile, CCT significantly overestimated RV volumes compared with the CMR values, resulting in a small but significant negative bias in the calculated RVEF. The patients in our cohort did not receive beta-blockers, because the use of beta-blockers is associated with significant

**Table 3** PFR by CCT compared to CMR ( $n=25$ )

	PRF-CT	PRF-MRI	Paired <i>t</i> test ( <i>p</i> )	Pearson's coefficient ( <i>r</i> )
PRF (%)	29.4±22.2	38.7±22.5	<0.001	0.90*

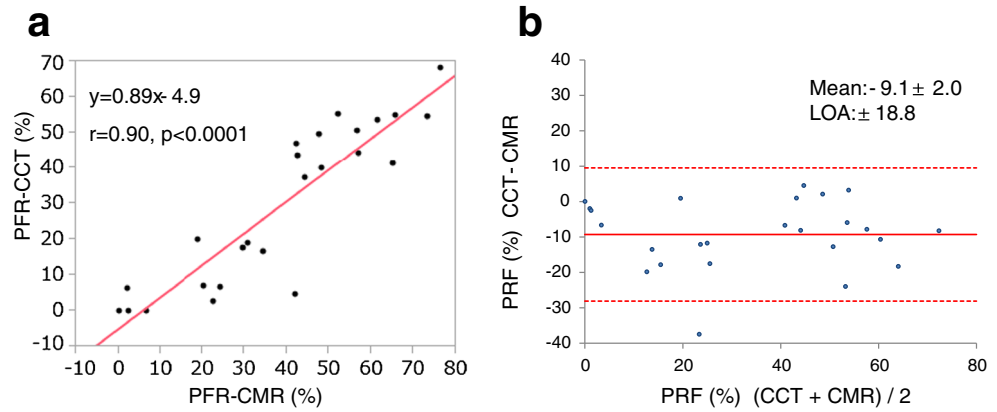
Data are mean±standard deviation; *n* = number of patients

PRF pulmonary regurgitant fraction

\* $p<0.0001$



**Fig. 8 a** Scattergram shows the results of linear regression analysis between PRF-CCT and PRF-CMR. **b** Bland–Altman plots show the degree of agreement between PRF-CCT and PRF-CMR. The *solid line* represents the mean difference. The *broken line* represents the 95 % limits of agreement (LOA) ( $\pm 1.96 \times SD$ ). The Bland–Altman analysis shows that CCT underestimated PRF compared with CMR



reductions in heart rate, SV and EF, and significant increases in ESV due to negative inotropic effects [16]. Therefore, the overestimations of EDV and SV for both LV and RV in our study might have been caused by transient increases in preload due to rapid inflow of contrast medium. In addition, 10 % steps for the reconstruction phase of CCT and interventricular dyssynchrony (RV contraction delay) often seen in repaired TOF patients might have missed the actual end-systolic point using CCT [17]. This might be considered a reason for the overestimation of RVESV and underestimation of RVEF. Alternative explanations could be the inter-modality differences in the ability to visualize endocardial boundary details and to include or exclude trabeculae that are prominent, especially in RVs from the ventricular cavity. Finally, these discrepancies between CCT and CMR measurements contributed to the lower regurgitant fraction derived by the CCT volumetric method compared with the CMR flow method, although methodological errors in either type of measurement could have also contributed to the difference. RV volume and the

severity of PR are often used as criteria for reoperation for pulmonary valve replacement (PVR) [4, 18–20], and the tendency for CCT to overestimate RV volume and underestimate PRF must be recognized. However, this tendency can be corrected by applying a fitting equation on input CCT variable: (1) RVEDV-CMR (ml) =  $0.87 \times \text{RVEDV-CCT (ml)} + 3.6$ , (2) RVESV-CMR (ml) =  $0.89 \times \text{RVESV-CCT (ml)} - 3.1$ , and (3) PRF-CMR (%) =  $0.91 \times \text{PRF-CCT (%)} + 11.8$ . The use of these fitting formulas obtained from two well-correlated data sets allows the prediction of RV functional parameters and PRF.

PRF-CCT obtained from bi-ventricular stroke volumes was excellently correlated with PRF-CMR obtained from phase-contrast MRI. The measurement of PRF by phase-contrast MRI has the limitation of susceptibility artefacts due to metallic implants in the RV outflow tract or pulmonary valve in patients with repaired TOF. In the present study, PRF-CMR could not be measured in three patients because of post-operative implants, and CT may circumvent this limitation of MRI. In addition, CCT is more useful than CMR in patients with intellectual impairment or congestive heart failure who cannot withstand long examination time in a supine position and repeated breath-hold in the examinational periods, because of a shorter imaging time with CT. The patients with PRF-CMR greater than 40 % were considered to have severe PR. The results of the present study demonstrated that a PRF-CMR of 40 % corresponds to a PRF-CCT of 31 %. In our study, 12 patients had PVR after CCT and CMR examination, and two of the 12 patients had cardiac function re-evaluated by CCT after PVR. Both patients had improved RV function, and PRF-CCT was reduced to nearly 0 %, as shown in Table 5.

As previously reported, CMR measurements of RV and LV function are highly reproducible in patients with both normal and dilated right ventricles [21]. In our study, the assessment of the reproducibility of the RV and LV function measurements showed that the CCT measurements had lower intra- and interobserver variability than CMR measurements. These findings indicate that CCT measurements of RV and LV function are highly reproducible in patients with repaired TOF. Lower

**Table 4** Inter- and intraobserver variability of RV and LV function obtained from repeated measurements by CCT and CMR in a subset of 15 randomly selected patients

	Interobserver variability (%)		Intraobserver variability (%)	
	CCT	CMR	CCT	CMR
RVEDV	3.5±2.8	5.3±6.2	3.4±3.1	6.2±4.9
RVESV	5.1±5.0	11.0±11.0	3.7±2.5	10.6±10.9
RVSV	7.5±5.6	8.2±7.3	5.5±5.2	8.5±10.5
RVEF	5.6±5.3	8.5±8.3	3.9±2.6	9.7±9.7
LVEDV	5.4±4.1	6.8±6.0	4.9±3.4	6.8±6.3
LVESV	7.3±6.8	9.6±7.2	7.6±5.4	9.5±6.7
LVSV	7.5±6.6	10.2±8.6	5.5±4.4	9.7±9.9
LVEF	4.5±3.9	5.2±5.8	5.1±2.7	6.8±4.3

Data are mean±standard deviation  
 CCT cardiac computed tomography, CMR cardiac magnetic resonance,  
 RV right ventricle, LV left ventricle, EDV end-diastolic volume, ESV end-systolic volume, SV stroke volume, EF ejection fraction

**Table 5** Comparison RV function between pre- and post- PVR by CCT

	Patient 1		Patient 2	
	Pre-operation	Post-operation	Pre-operation	Post-operation
RVEDV (ml/m <sup>2</sup> )	269.0	154.4	174.9	125.1
RVESV (ml/m <sup>2</sup> )	192.1	104.0	99.2	76.2
RVSV (ml/m <sup>2</sup> )	76.9	50.5	75.7	48.9
RVEF (%)	28.6	32.7	43.3	39.1
PRF-CT (%)	55.0	0	47.0	3.6

RV right ventricle, EDV end-diastolic volume, ESV end-systolic volume, SV stroke volume, EF ejection fraction, PRF pulmonary regurgitant fraction

variability values of CCT measurements compared with CMR measurements may be related to better definition of contours obtained from the high spatial resolution of CT. In repaired TOF patients who have large RV volumes, the RV cavity becomes more spherical and this makes it easier to define the boundary of the intracavitary lumen; however, the shape of LV cavity may become distorted because of exclusion by the large RV volume. These changes might have helped to reduce the intra- and interobserver variability in the RV functional parameters in our patient cohort.

The disadvantages of CCT compared with CMR include radiation exposure and the need to use contrast material, which may lead to allergic reactions or kidney damage. Most CCT protocols currently used for the evaluation of ventricular function utilize retrospective ECG-gating, which can result in a substantial radiation exposure of about 14.8–21.1 mSv [22–24]. Recently, retrospective ECG-gated CCT performed with iterative reconstruction and low tube voltage allowed a reduction in the radiation dose while maintaining image quality and the accuracy of functional analysis [25, 26]. Our CT protocol in combination with iterative reconstruction and low tube voltage could reduce the effective radiation dose (mean, 7.6 mSv) by 50 % of the amount typically required for retrospective ECG-gating. Patients with repaired TOF are younger than patients with ischemic cardiomyopathy, and they must receive repetitive cardiac examination; therefore, low dose radiation exposure is necessary.

Furthermore, we used the split-bolus injection with diluted contrast media to obtain an accurate contour of the inner margin of the RV cavity [27, 28]. It provided sufficient attenuation for visualization of the right heart, and the right heart structures could be seen clearly. This probably reduced the time required for ventricular volume measurements by CCT.

Our study has several limitations. First, the size of the study population was rather small. Second, our study did not compare volumetric data and pulmonary regurgitation with measurements obtained by cardiac catheterization. Finally, using 10 % steps for the reconstruction phase and acquisition during 10–90 % of RR interval on CCT measurements could potentially affect the determination of the actual end-diastolic and end-systolic phases.

In conclusion, ECG-gated 256-slice CCT can assess the RV and LV function, and PRF with high reproducibility in patients with repaired TOF; and the combination of low tube voltage and an iterative reconstruction technique lowers that radiation dose exposure by as much as 50 %. RV and LV functional parameters, and PRF obtained from CCT are excellently correlated with those from CMR in patients with repaired TOF. Although the tendency for CCT to overestimate RV volume and underestimate PRF was observed, CCT measurements can be corrected by applying the fitting formulas from excellent correlations between CCT and CMR parameters.

**Acknowledgements** The scientific guarantor of this publication is Hiroshi Honda. The authors of this manuscript declare relationships with the following companies: Nagao M. and Kawanami S: Bayer Healthcare Japan, Modest, Research Grant; Philips Electronics Japan, Modest, Research Grant

Higuchi K.: Philips Electronics Japan, Employee. This study has received funding by the Japan Society for the Promotion of Science (JSPS) KAKENHI (25461831). No complex statistical methods were necessary for this paper. Institutional review board approval was obtained. Written informed consent was obtained from all subjects (patients) in this study. Methodology: prospective, diagnostic study, performed at one institution.

## References

1. van Straten A, Vliegen HW, Hazekamp MG et al (2004) Right ventricular function after pulmonary valve replacement in patients with tetralogy of Fallot. *Radiology* 233:824–829
2. Oechslin EN, Harrison DA, Harris L et al (1999) Reoperation in adults with repair of tetralogy of fallot: indications and outcomes. *J Thorac Cardiovasc Surg* 118:245–251
3. Ammash NM, Dearani JA, Burkhart HM, Connolly HM (2007) Pulmonary regurgitation after tetralogy of Fallot repair: clinical features, sequelae, and timing of pulmonary valve replacement. *Congenit Heart Dis* 2:386–403
4. Lee C, Kim YM, Lee CH et al (2012) Outcomes of pulmonary valve replacement in 170 patients with chronic pulmonary regurgitation after relief of right ventricular outflow tract obstruction: implications for optimal timing of pulmonary valve replacement. *J Am Coll Cardiol* 60:1005–1014
5. Mercer-Rosa L, Yang W, Kutty S, Rychik J, Fogel M, Goldmuntz E (2012) Quantifying pulmonary regurgitation and right ventricular

- function in surgically repaired tetralogy of Fallot: a comparative analysis of echocardiography and magnetic resonance imaging. *Circ Cardiovasc Imaging* 5:637–643
6. Michaely HJ, Nael K, Schoenberg SO et al (2006) Analysis of cardiac function—comparison between 1.5 Tesla and 3.0 Tesla cardiac cine magnetic resonance imaging: preliminary experience. *Invest Radiol* 41:133–140
  7. Lotz J, Doker R, Noeske R et al (2005) In vitro validation of phase-contrast flow measurements at 3 T in comparison to 1.5 T: precision, accuracy, and signal-to-noise ratios. *J Magn Reson Imaging* 21: 604–610
  8. Gutberlet M, Noeske R, Schwinge K, Freyhardt P, Felix R, Niendorf T (2006) Comprehensive cardiac magnetic resonance imaging at 3.0 Tesla: feasibility and implications for clinical applications. *Invest Radiol* 41:154–167
  9. Takx RA, Moscariello A, Schoepf UJ et al (2012) Quantification of left and right ventricular function and myocardial mass: comparison of low-radiation dose 2nd generation dual-source CT and cardiac MRI. *Eur J Radiol* 81:e598–e604
  10. Seneviratne SK, Truong QA, Bamberg F et al (2010) Incremental diagnostic value of regional left ventricular function over coronary assessment by cardiac computed tomography for the detection of acute coronary syndrome in patients with acute chest pain: from the ROMICAT trial. *Circ Cardiovasc Imaging* 3:375–383
  11. Maffei E, Messalli G, Martini C et al (2012) Left and right ventricle assessment with cardiac CT: validation study vs. cardiac MR. *Eur Radiol* 22:1041–1049
  12. Guo YK, Gao HL, Zhang XC, Wang QL, Yang ZG, Ma ES (2010) Accuracy and reproducibility of assessing right ventricular function with 64-section multi-detector row CT: comparison with magnetic resonance imaging. *Int J Cardiol* 139:254–262
  13. Alfakih K, Plein S, Bloomer T, Jones T, Ridgway J, Sivananthan M (2003) Comparison of right ventricular volume measurements between axial and short axis orientation using steady-state free precession magnetic resonance imaging. *J Magn Reson Imaging* 18:25–32
  14. Ochiai R, Yao A, Kinugawa K, Nagai R, Shiraishi I, Niwa K (2011) Status and future needs of regional adult congenital heart disease centers in Japan. *Circ J* 75:2220–2227
  15. Marelli AJ, Mackie AS, Ionescu-Ittu R, Rahme E, Pilote L (2007) Congenital heart disease in the general population: changing prevalence and age distribution. *Circulation* 115:163–172
  16. Jensen CJ, Jochims M, Hunold P et al (2010) Assessment of left ventricular function and mass in dual-source computed tomography coronary angiography: influence of beta-blockers on left ventricular function: comparison to magnetic resonance imaging. *Eur J Radiol* 74:484–491
  17. Mueller M, Rentzsch A, Hoetzer K et al (2010) Assessment of interventricular and right-intraventricular dyssynchrony in patients with surgically repaired tetralogy of Fallot by two-dimensional speckle tracking. *Eur J Echocardiogr* 11:786–792
  18. Geva T (2011) Repaired tetralogy of Fallot: the roles of cardiovascular magnetic resonance in evaluating pathophysiology and for pulmonary valve replacement decision support. *J Cardiovasc Magn Reson* 13:9
  19. Warnes CA, Williams RG, Bashore TM et al (2008) ACC/AHA 2008 guidelines for the management of adults with congenital heart disease: a report of the American College of Cardiology/American Heart Association Task Force on Practice Guidelines (writing committee to develop guidelines on the management of adults with congenital heart disease). *Circulation* 118:e714–e833
  20. Baumgartner H, Bonhoeffer P, De Groot NM et al (2010) ESC guidelines for the management of grown-up congenital heart disease (new version 2010). *Eur Heart J* 31:2915–2957
  21. Mooij CF, de Wit CJ, Graham DA, Powell AJ, Geva T (2008) Reproducibility of MRI measurements of right ventricular size and function in patients with normal and dilated ventricles. *J Magn Reson Imaging* 28:67–73
  22. Earls JP, Berman EL, Urban BA et al (2008) Prospectively gated transverse coronary CT angiography versus retrospectively gated helical technique: improved image quality and reduced radiation dose. *Radiology* 246:742–753
  23. Maruyama T, Takada M, Hasuike T, Yoshikawa A, Namimatsu E, Yoshizumi T (2008) Radiation dose reduction and coronary assessability of prospective electrocardiogram-gated computed tomography coronary angiography: comparison with retrospective electrocardiogram-gated helical scan. *J Am Coll Cardiol* 52:1450–1455
  24. Hausleiter J, Meyer T, Hadamitzky M et al (2006) Radiation dose estimates from cardiac multislice computed tomography in daily practice: impact of different scanning protocols on effective dose estimates. *Circulation* 113:1305–1310
  25. Hou Y, Liu X, Xv S, Guo W, Guo Q (2012) Comparisons of image quality and radiation dose between iterative reconstruction and filtered back projection reconstruction algorithms in 256-MDCT coronary angiography. *AJR Am J Roentgenol* 199:588–594
  26. Oda S, Utsunomiya D, Funama Y et al (2011) A low tube voltage technique reduces the radiation dose at retrospective ECG-gated cardiac computed tomography for anatomical and functional analyses. *Acad Radiol* 18:991–999
  27. Kerl JM, Ravenel JG, Nguyen SA et al (2008) Right heart: split-bolus injection of diluted contrast medium for visualization at coronary CT angiography. *Radiology* 247:356–364
  28. Kondo M, Nagao M, Yonezawa M et al (2014) Improvement of automated right ventricular segmentation using dual-bolus contrast media injection with 256-slice coronary CT angiography. *Acad Radiol* 21:648–653